Gas Turbine Casing Response to Blade Vibrations: Analytical and Experimental results

Publication details:
Sixth DSTO International Conference on Health & Usage Monitoring
978-0-9803215-6-2 (ISBN)

Event details:
Sixth DSTO International Conference on Health & Usage Monitoring
Melbourne, Australia

Publication Date:
2009

DOI:
https://doi.org/10.26190/unsworks/471

Gas Turbine Casing Response to Blade Vibrations: Analytical and Experimental results

Gareth L. Forbes, Robert B. Randall

School of Mechanical and Manufacturing Engineering, University of New South Wales, Sydney, NSW, 2052, Australia

Abstract

The non-intrusive measurement of blade condition within a gas turbine would be a significant aid in the maintenance and continued operation of these engines. Online condition monitoring of the blade health by non-contact measurement methods is obviously the ambition of most techniques, with a number of methods proposed, investigated and employed for such measurement. The current dominant method uses proximity probes to measure blade arrival time for subsequent processing. It has been recently proposed however, that measurement of the turbine casing vibration response could provide a means of blade condition monitoring. The casing vibration is believed to be excited pre-dominantly by (i) the moving pressure waveform around each blade throughout its motion and (ii) the moments applied by the stationary stator blades. Any changes to the pressure profile around the rotating blades, due to their vibration, will therefore in turn affect these excitation forces.

Previous work has introduced an analytical model of a gas turbine casing, and simulated pressure signal associated with the rotating blades. The model has been extended in this paper to more closely represent a commercial gas turbine with experimental verification being presented for various aspects of the analytical modelling procedure.

Keywords: Gas turbines, forced response, casing vibrations, rotor blade vibrations.

Introduction

The internal components of gas turbines operate under the extreme conditions of high stress and temperatures. The main working surfaces inside a turbine engine encountering these conditions are the multiple rotor and stator blade rows. It is of no surprise that analysis of the stress and heat transfer ability of these components has continually been subject to research and development to improve engine design and operating life.

Measurement and modelling of blade vibrations has developed for two main applications, determination of stress levels induced by the blades' dynamic motion and to quantify blade condition. Analytical [1] and more recently computational [2] models have been developed to determine forced blade motion and stresses taking into account effects such as; wake passing, blade tip vortices as well as structural and aerodynamic loadings on blades.

The current dominant blade vibration measurement method, in the aero-industry [3, 4], during the engine development phase, is blade tip timing (BTT). BTT is achieved through proximity probe measurements obtaining the arrival time of blades at different points around the casing periphery. BTT methods are currently able to satisfactorily measure asynchronous, non-integer multiples of shaft speed, and blade vibrations due to rotating stall, flutter and compressor surge, but require two transducers, perforating the casing, for each blade row. However, no single method is able to fully characterise the vibration parameters of blades in service [5].

An alternative method has been proposed for non-intrusive measurements of blade vibrations by means of external accelerometer measurements on the casing of a gas turbine [6-8]. Investigation into the response of a turbine casing under the influence of operating pressure

conditions was first undertaken in [9], with the correlation between measured internal pressure signals and casing vibration measurements shown. Further investigations by the same author have been conducted into the use of unsteady wall pressure signals for blade fault identification in [10] with the extension to CFD simulation of blade faults in [11, 12]. The preceding works have dealt solely with the deterministic periodic forced vibrations. It is thought this is driven by the fact that it is these periodic forces that usually are the most destructive forces within an engine and can cause large deflections and blade stresses. It is however well understood that the operating conditions inside a gas turbine are highly turbulent, due to a wide variety of influences including but not limited to; ingested turbulence, turbulent boundary layer flow, wake interaction, reversed flow and tip vortex flow.
Measurements of the casing wall pressure and vibration signal have been taken from a simplified experimental turbine test rig and are presented within this paper. An analytical simulation of the internal pressure signal is also compared to the experimental measurements. Although the aim of this study is to highlight the ability to obtain blade vibration information from casing vibrations, a comparison between the measured and analytic signal is primarily done on the pressure signal. Both wall pressure and casing vibration signals should contain the same essential information, which will be discussed further in later sections, however in this case the measurement and interpretation of the pressure signal is less complex than the casing vibration response measurements. Conversely in practice, the ease of making pressure measurements is much less than for accelerometer measurements, since pressure transducers require perforation of the casing and operate in a much harsher environment. Furthermore, the analysis and results within this paper deal predominantly with the effects of the random fluctuations on the mean periodic flow, and it is shown that after separation of the dominant periodic components that the stochastic portion of the pressure and casing measurements contains key information on blade vibrations.

Pressure Generation

Flow over the rotor and stator blade aerofoils in a turbine causes high and low pressure forces to act over the blade surfaces. These high and low pressure profiles then interact as the pressure distributions around the rotor blades rotate around, causing fluctuating pressures on the casing surface, as well as interacting with the stationary pressure profiles around the stator blades. Shown schematically in Fig. 1 is the first harmonic of the pressure profile around a set of rotor blades. It can be seen that the pressure on the surface of the casing will therefore vary harmonically with the rate at which blades pass that point, i.e. the blade passing frequency, BPF.

Blade forced response

It has been stated at the beginning of this section that the pressure profiles around both the stator and rotor blades will cause a fluctuating pressure on the surface of the casing due to blade passing frequency. Additionally as the rotor blades rotate around the engine they will in turn also be influenced by the varying pressure profile and wakes from the trailing edges of leading stator rows, schematically shown in Fig. 2. The fluctuating forces on the rotor blades will now cause them to vibrate due to the fluctuating pressure, which is driven at the rate which the rotor blades pass through this changing pressure field, i.e. stator passing frequency, SPF.

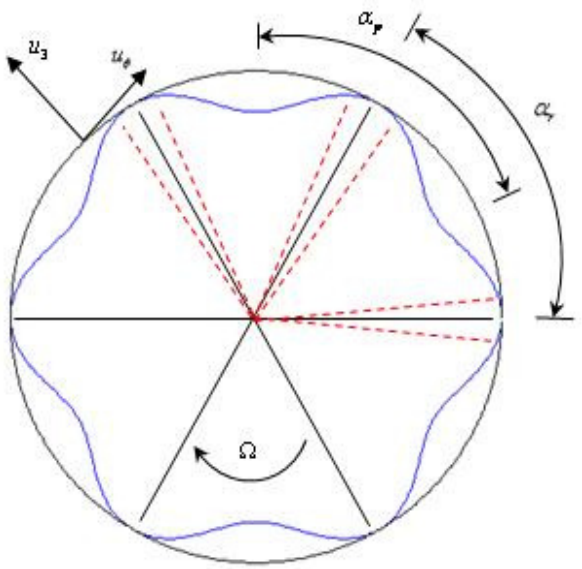

Fig. 1 Cross sectional schematic of turbine casing, blades and pressure profiles. The dashed lines represent blade motion. Note: only 6 blades shown

The pressure acting on rotor blades downstream of a stator blade row has been shown to have, in general, a damped impulse shape [13] (obviously this varies widely and is dependent on the specific turbine). Turbo-machinery flow conditions are however inherently turbulent, with background turbulence intensity levels often reported to be approx. 3-4%, and turbulence within the wake region often five times greater than the background turbulence [14, 15]. It is also noted that the frequency content of turbulence within a gas turbine will be somewhat band-limited; however in the context of this work the turbulence was assumed to be completely broadband.

The forces acting on the rotor blades are therefore modelled as a raised cosine with a period of half the stator blade passing frequency, refer to Fig. 3, and modulated by random fluctuations due to turbulence. The Fourier series expansion of the force on the 'r^{th}' blade can be expressed as:

$$f(t)_r = F_0\left(b(t)+1\right)\left\{\sum_{i=0}^{\infty} A_i \cos\left[i\left(\omega_{spf} t+\gamma_r\right)\right]\right\} \tag{1}$$

$$\gamma_r = \frac{2\pi s(r-1)}{b} - \text{round}\left(\frac{s(r-1)}{b}\right)2\pi \tag{2}$$

where A_i are the Fourier coefficients, ω_{spf} is the stator passing frequency, $b(t)$ is the uniformly distributed random variable with a zero mean and a deviation of $\pm 7.5\%$, with s the number of stator blades and b the number of rotor blades.

The rotor blades are modelled as a simple oscillator, i.e. a single degree of freedom spring mass damper system being an adequate model for blades with well separated modes [16]. Only the solution for the stochastic portion of both the blade motion and pressure force will be obtained in this study for brevity; this is also the portion of the signal that contains the most useful information. Derivation of the solution for the deterministic portion can however be found in [6].

The solution for the motion of the 'r^{th}' blade can therefore be shown to be:

$$X(f)_r = H(f)_r F(f)_r \tag{3}$$

where capitalization refers to the Fourier transform of the corresponding time signal and $H(f)_r$ is the transfer function of the 'r^{th}' blade being:

$$H(f)_r = \frac{A_r}{\left(\omega_{nb}^2 - \omega^2\right) + 2\zeta_2 j\omega_{nb}\omega} \tag{4}$$

A_r being the gain factor for the 'r^{th}' blade.

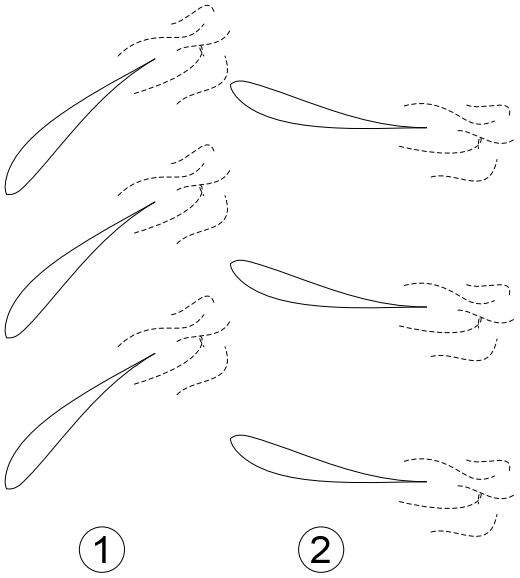

Fig. 2 Wake interaction between stator (1) and rotor (2) blade rows

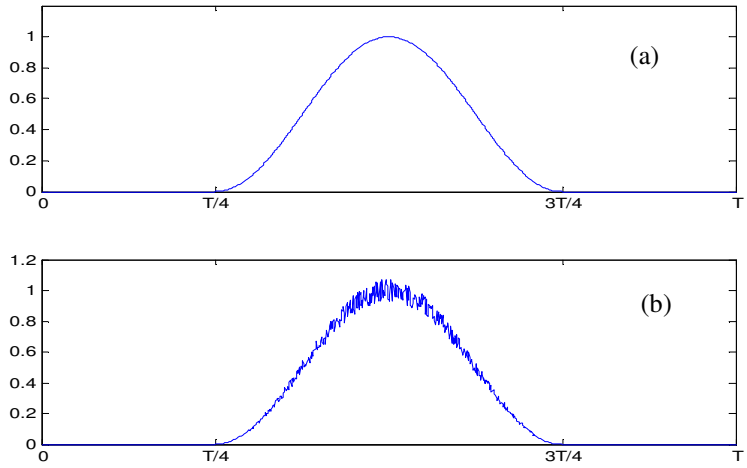

Fig. 3 blade forcing function, purely deterministic (a), with random fluctuations (b)

Pressure on casing surface

The pressure generated on the casing surface will be affected by the motion of the blade. This will now cause the pressure around the rotor blades to vary due to the blade motion, with the blade pressure profile following the blade motion as it vibrates about its equilibrium position. The pressure from the 'r^{th}' blade is once again modelled as a raised cosine with half a period of one rotor blade spacing, with the Fourier expansion given as:

$$P_r = \sum_{i=0}^{\infty} A_i.P.e^{ji\left[\theta - \Omega t - x(t)_r - \alpha_r\right]} \tag{5}$$

Note that Eqn. (5) is a rotating sinusoidal pressure with the phase modulated by the blade motion $x(t)$.

Experimental Setup and Measurement

The test rig consists of a 19 flat blade rotor arrangement driven by an electric motor which is currently capable of running at speeds up to 2500rpm. A toroidal ring in front of the bladed arrangement, supplied with high pressure air, provides six jets which act like trailing edge flow from upstream stator blade rows exciting the rotor blades at multiples of shaft speed. A microphone and accelerometer are located in the vertical plane above the blade on the casing. Measurements were taken with a shaft rotational speed of 2000 rpm, and analyzer sampling rate of 65.536 kHz of which the useful frequency range is 25.6 kHz.

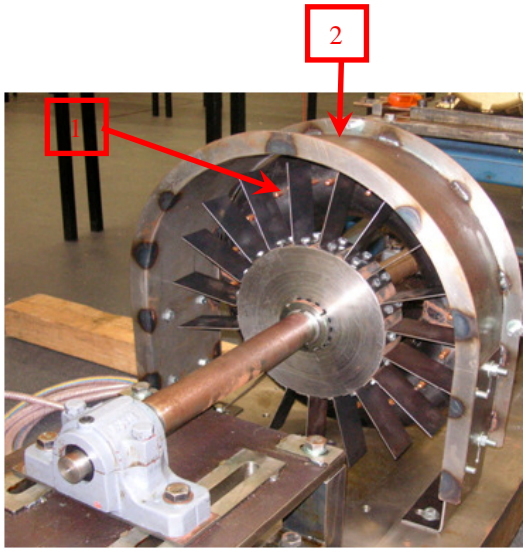

Fig. 4 Experimental test rig. (1) Air jets located on a toroidal ring which is supplied with high pressure air. (2) location of microphone and accelerometer mounting.

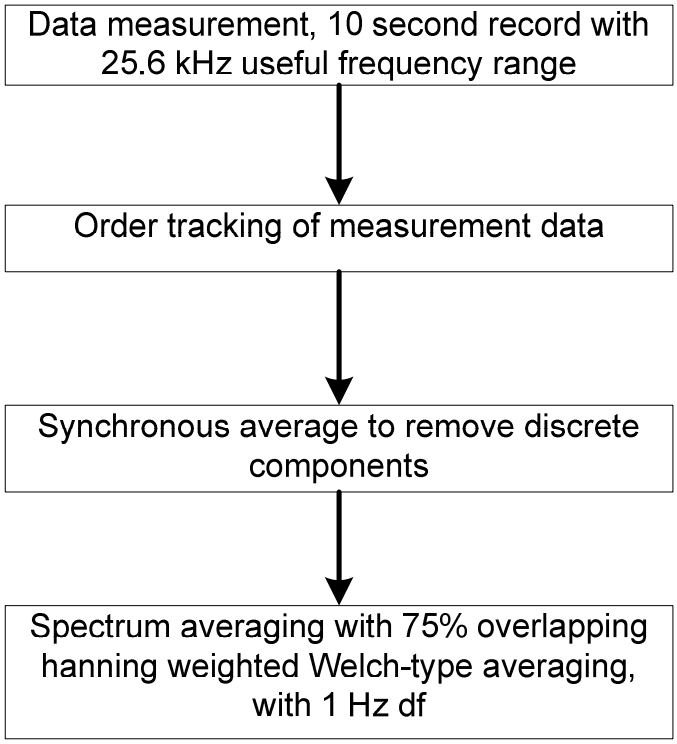

Fig. 5 Flowchart of measurement post processing

Shown in Fig. 5 is the flow chart of the data measurement and post processing of the measured signal. The measured signal was re-sampled in the angular domain with an integer number of

samples per revolution, triggered by a measured once per-rev tacho signal, often referred to as order tracking. This has the advantage that the re-sampled signal can have fluctuations due to changes in shaft speed easily removed. This is done by time domain synchronous averaging the order tracked signal, with a period equal to shaft speed this also allows separation of the discrete and random components. The power spectrum was then calculated using a hanning weighted, 75% overlapping, Welch-type averaging, resulting in a spectrum with 1 Hz frequency resolution.

Results

Experimental results were obtained for an input shaft speed of 2000 rpm, with measurement of casing wall pressure, casing acceleration and tacho signal. Analytical results are also shown for the simulated pressure signal, for the same operating conditions as the experimental test rig; i.e. 19 rotor blades, 6 stator blades, and 2000rpm shaft speed.
The power spectrum, over a limited range of the measured pressure and acceleration signals can be seen in Fig. 6. The residual signal is overlaid on the synchronously averaged discrete signal. The discrete signals can be seen to be made up of multiple discrete peaks at harmonics of shaft speed, with the largest peak at a multiple of BPF. The residual signal in Fig. 6(a) can be seen to be relatively flat with double peaks either side of multiples of shaft speed, the zoomed spectrum in Fig. 7 shows this more clearly. The same overall structure of the residual signal is apparent in the casing vibration signal, with the addition of broad structural resonance peaks, indicated by the arrows. This is the fundamental difference in the results which are seen between the pressure and casing vibration signals. This is owing to the fact that the casing vibrations are driven by the internal pressure force, so the casing vibrations should resemble the pressure signal after it has passed through the structural transfer function, a Linear Time Invariant Filter.

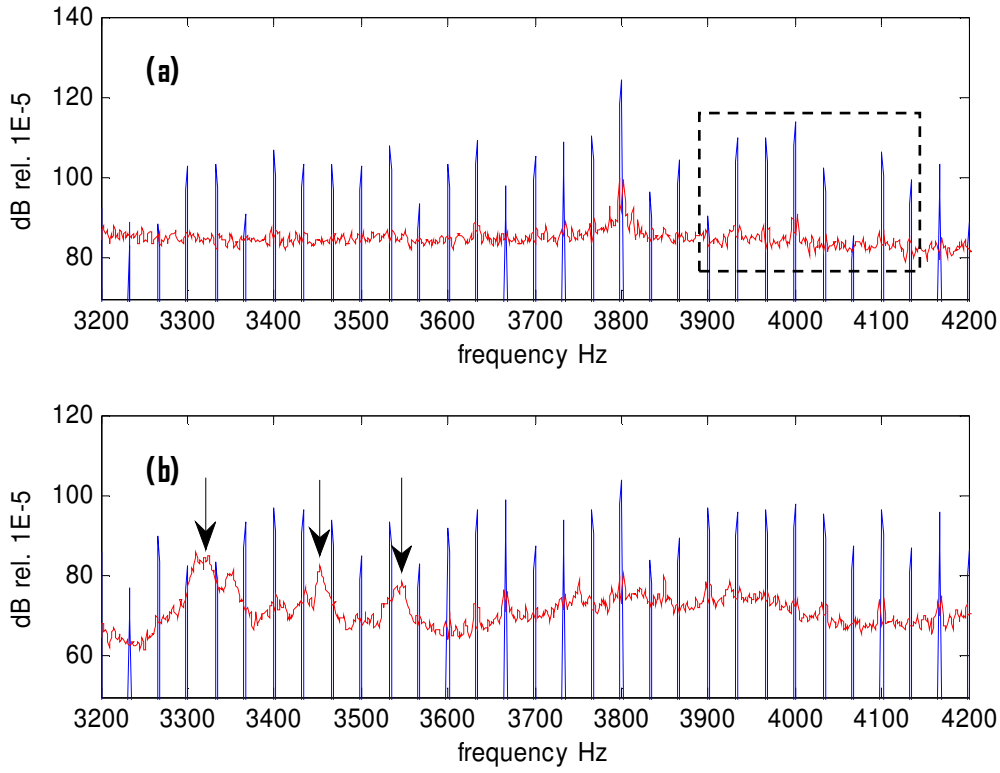

Fig. 6 (a) PSD of measured pressure signal, separated discrete and residual signal overlaid on each other, (b) measured casing acceleration signal. Arrows indicate the structural resonance peaks in the acceleration signal.

The zoomed spectrum shown in Fig. 7, highlights the narrow band peaks centred around multiples of shaft speed. Shown by the solid vertical lines are the 118 – 125 multiples of shaft speed, the other vertical dashed lines show the corresponding half multiples of shaft speed ± the blade natural frequency, ie. 118.5 – 125.5 ± blade natural frequency.

There is a discrepancy between the measured pressure signal and that which is modelled in accordance with the earlier derived pressure signal. Fig. 8 shows the simulated pressure signal, which contains the same sets of two narrow band peaks. However they are shifted by an amount of half shaft speed, i.e. they are centred around whole numbers of shaft speed; shown is 118 – 125 times shaft speed ± blade natural frequency. It is believed this difference can be explained by discrete frequencies which exist at half multiples of shaft speed in the experimental results, as seen in Fig. 9. The discrete frequencies in Fig. 9 are extracted by taking the synchronous average of the angular re-sampled signal at double the shaft speed period. As can be seen in Fig. 9 the half shaft speed harmonic and particularly the one and a half shaft speed harmonic are of the same order as the integer multiples of shaft speed. The existence of these half order discrete shaft order harmonics, presumably caused by parametric excitation, could then cause this modulation, or half shaft speed shift which is not at present allowed for in the theoretical model.

Despite the differences between the results, the important ability to determine the blade natural frequency is still able to be established, which can be estimated by the space between these two narrow peaks. The difference between the two narrow peaks can be shown to be:

$$diff = 2 \times Blade\,nat.f - q\Omega \tag{6}$$

The value of 'q' can be found by plotting the diff value verses 'q' and observing where the plot passes through zero. This however requires knowledge of the blade natural frequency to at least within shaft speed.

In these results, the space is on average 5 Hz, and the blade natural frequency is known to be around 117 Hz, from measurements taken while the shaft is stationary [17]. A blade natural frequency can thus be calculated to be approximately 119 Hz. This corresponds well with the expected increase in natural frequency which would result from centrifugal stiffening.

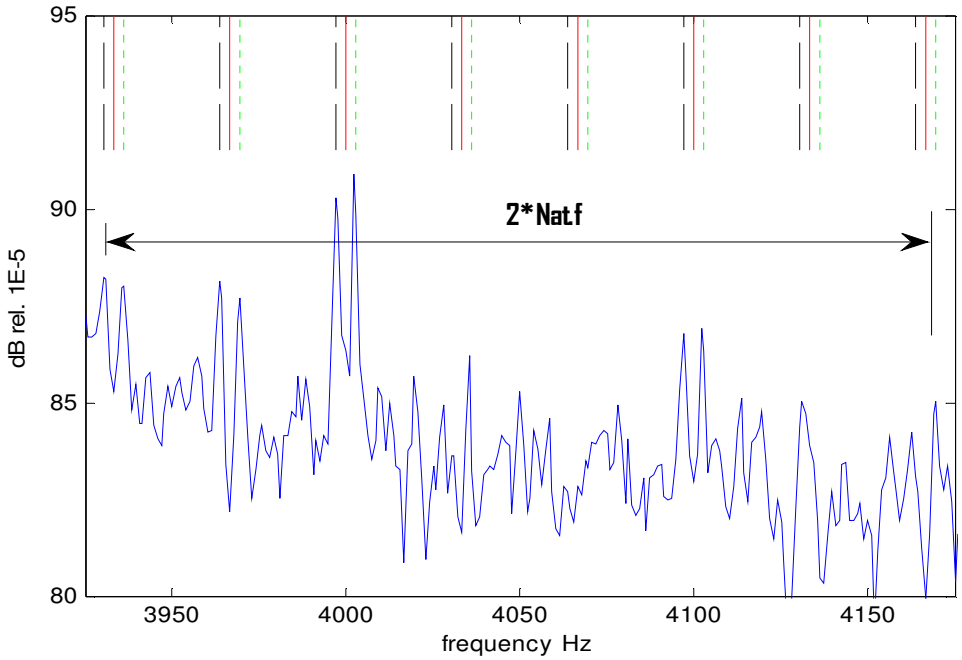

Fig. 7 Zoomed spectrum of the measured residual pressure signal. Vertical —— line at shaft speed spacing, vertical - - - - line at shaft speed – blade natural frequency, vertical ····· line at shaft speed + blade natural frequency

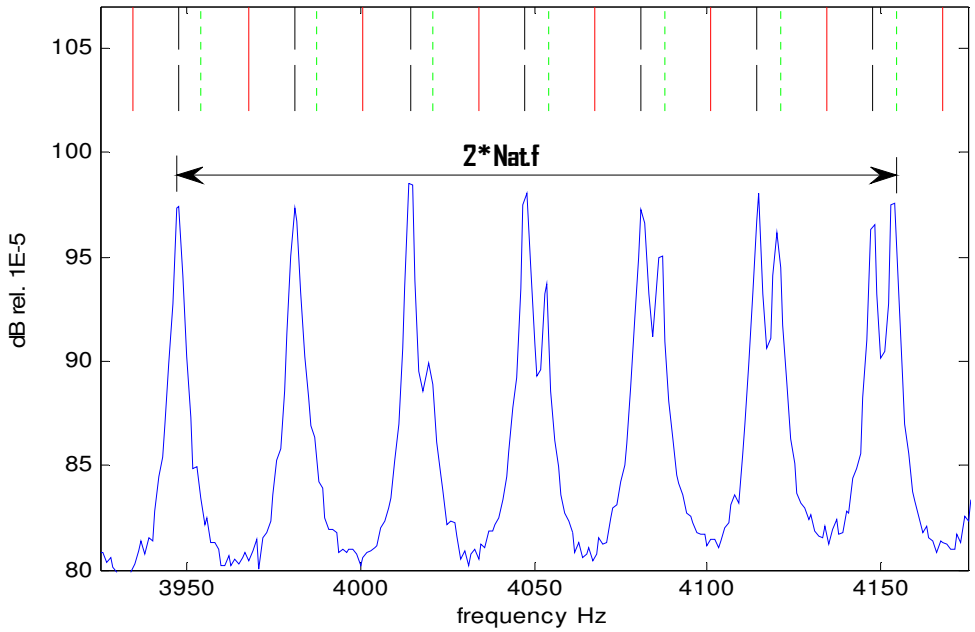

Fig. 8 Zoomed spectrum of the analytic residual pressure signal. Vertical ——— line at shaft speed spacing, vertical - - - - line at shaft speed – blade natural frequency, vertical ····· line at shaft speed + blade natural frequency.

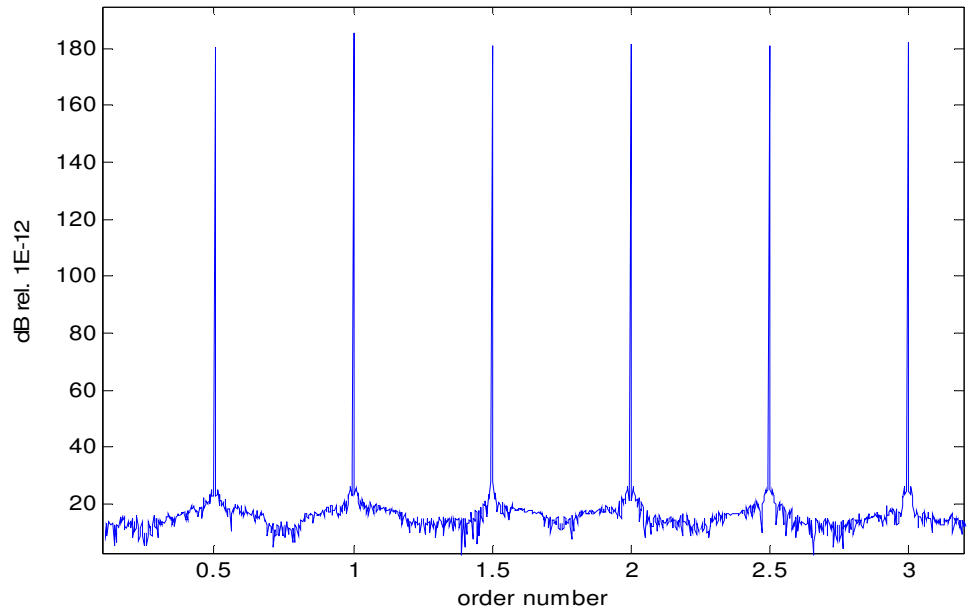

Fig. 9 Spectrum of the discrete synchronous average components, with synchronous average length twice shaft speed length

Conclusions

Measured casing wall pressure and casing vibrations have been presented along with the analytical formulations of the internal pressure signal for a simplified turbine test rig. Results for the simulated pressure signal shown here and in previous work [7, 8] have been shown to contain the same signal features as those which have been measured, namely; discrete peaks at multiples of shaft speed and narrow band peaks at multiples of shaft speed ± blade natural frequency, although there currently exists a half shaft speed frequency shift between the two results which is thus far not fully explained. Despite this discrepancy, the important feature of

being able to estimate the blade natural frequency from wall pressure measurements or casing vibrations is still able to be achieved.

Acknowledgements

Grateful acknowledgment is made for the financial assistance given by the Australian Defence Science and Technology Organisation, through the Centre of Expertise in Helicopter Structures and Diagnostics at UNSW.

References

1. Majjigi, R.K. and P.R. Gliebe, *Development of rotor wake/vortex model*, in *NASA-CR-174849*. 1984, NASA contract NAS3-23681.
2. Chiang, H.-W.D. and R.E. Kielb, *Analysis system for blade forced response.* Journal of Turbomachinery, Transactions of the ASME, 1993. **115**(4): p. 762-770.
3. Zielinski, M. and G. Ziller, *Noncontact Blade Vibration Measurement System for Aero Engine Application.* American Institute of Aeronautics and Astronautics, 2005(ISABE).
4. Heath, S., *A New Technique for Identifying Synchronous Resonances Using Tip-Timing.* Journal of Engineering for Gas Turbines and Power, 2000. **122**(2): p. 219-225.
5. Heath, S., et al. *Turbomachinery blade tip measurement techniques*. in *Advanced Non-Intrusive Instrumentation for Propulsion Engines*. 1997. Brussels, Belgium.
6. Forbes, G.L. and R.B. Randall. *Simulated Gas Turbine Casing Response to Rotor Blade Pressure Excitation*. in *5th Australasian Congress on Applied Mechanics*. 2007. Brisbane, Australia.
7. Forbes, G.L. and R.B. Randall. *Separation of excitation forces from simulated gas turbine casing response measurements*. in *EURODYN 2008*. 2008. Southampton, UK.
8. Forbes, G.L. and R.B. Randall. *Detection of a Blade Fault from Simulated Gas Turbine Casing Response Measurements*. in *4th European Workshop on Structural Health Monitoring* 2008. Krakow, Poland.
9. Mathioudakis, K., E. Loukis, and K.D. Papailiou. *Casing vibration and gas turbine operating conditions*. 1989. Toronto, Ont, Can: Publ by American Soc of Mechanical Engineers (ASME), New York, NY, USA.
10. Mathioudakis, K., et al., *Fast response wall pressure measurement as a means of gas turbine blade fault identification.* Journal of Engineering for Gas Turbines and Power, Transactions of the ASME, 1991. **113**(2): p. 269-275.
11. Dedoussis, V., K. Mathioudakis, and K.D. Papiliou. *Numerical simulation of blade fault signatures from unsteady wall pressure signals*. 1994. Hague, Neth: Publ by ASME, New York, NY, USA.
12. Stamatis, A., N. Aretakis, and K. Mathioudakis. *Blade fault recognition based on signal processing and adaptive fluid dynamic modelling*. 1997. Orlando, FL, USA: ASME, New York, NY, USA.
13. Mailach, R., L. Muller, and K. Vogeler, *Rotor-stator interactions in a four-stage low-speed axial compressor - Part II: Unsteady aerodynamic forces of rotor and stator blades.* Journal of Turbomachinery, 2004. **126**(4): p. 519-526.
14. Henderson, A.D., G.J. Walker, and J.D. Hughes, *The influence of turbulence on wake dispersion and blade row interaction in an axial compressor.* Journal of Turbomachinery, 2006. **128**(1): p. 150-157.
15. Dullenkopf, K. and R.E. Mayle, *Effects of incident turbulence and moving wakes on laminar heat transfer in gas turbines.* Journal of Turbomachinery, Transactions of the ASME, 1994. **116**(1): p. 23-28.
16. Dimitriadis, G., et al., *Blade-tip timing measurement of synchronous vibrations of rotating bladed assemblies.* Mechanical Systems and Signal Processing, 2002. **16**(4): p. 599-622.
17. Clark, M., *Turbine Blade Diagnostics*, in *School of Mechanical and Manufacturing Engineering*. 2006, University of New South Wales: Sydney.